Journal of Alloys and Compounds 509 (2011) 9572–9576

Contents lists available at ScienceDirect

Journal of Alloys and Compounds

journal homepage: www.elsevier.com/locate/jallcom

A theoretical analysis of zero-field splitting parameters of Mn^{2+} doped dicadmium diammonium sulfate $Cd_2(NH_4)_2(SO_4)_3$ single crystal

Muhammed Açıkgöz *

Faculty of Arts and Sciences, Bahcesehir University, Beşiktaş 34353, İstanbul, Turkey

ARTICLE INFO

Article history:
Received 18 April 2011
Received in revised form 19 July 2011
Accepted 21 July 2011
Available online 28 July 2011

Keywords:
Spin Hamiltonians
Crystal structure
Crystal and ligand fields
Mn^{2+}

ABSTRACT

The superposition model (SPM) and crystallographic data are utilized to determine the zero-field splitting (ZFS) parameters (ZFSPs) for Mn^{2+} ions in $Cd_2(NH_4)_2(SO_4)_3$ single crystal, assuming that the Mn^{2+} ions locate at either Cd^{2+} or NH^{4+} site. The SPM results has been verified by the fourth-order perturbation formulae analysis. Experimental suggestions about Mn^{2+} ions substituting at Cd^{2+} sites have been confirmed theoretically for the first time.

1. Introduction

Dicadmium diammonium sulfate $Cd_2(NH_4)_2(SO_4)_3$ crystal, abbreviated as CAS hereafter, is one of the langbeinite-type crystals having the general formula $X_2Y_2(SO_4)_3$, where X is a divalent metal, e.g. Cd, Zn, Mg, Ca and Y is ammonium (NH_4) or a monovalent metal, e.g. K, Tl, Rb, Cs [1,2]. CAS has been the subject of many investigations [3–10] since its discovery by Jona and Pepinsky [3]. The ferroelectricity of CAS below 90 K was found out as well [3]. The disordering of the SO_4 ion in the high temperature phase was suggested based on Raman, infrared and far-infrared studies since no mode softening was observed [4]. Electron paramagnetic resonance (EPR) investigations of Mn^{2+} doped CAS single-crystal were reported in [5–7]; first at room temperature [5], whereas more detailed study [6] included also the crystal structure of Mn^{2+}:CAS. No change in space group symmetry at 80 K could be observed [6], in spite of the fact that a monoclinic ferroelectric phase of CAS below 90 K was suggested [2,3]. The structural phase transitions in CAS were studied by EPR in [7] and [8,9]. The studies [7–10], reporting a proton NMR, indicated some dynamical disordered arrangements related to ammonium and sulfate ions. Also, the authors [7] suggested that the phase transition occurred because of the freezing of the sulfate rotations, while the structural change was considered as a result of some motional change of the sulfate group in [6]. The zero-field splitting (ZFS) parameters (ZFSPs) of Mn^{2+} in CAS were measured by EPR at room temperature [5–7].

In the present paper, first theoretical analysis of the ZFSPs of Mn^{2+} ions in CAS has been carried out. The ZFSPs have been calculated for different paramagnetic centers formed by Mn^{2+} ions at possible sites, namely, Cd^{2+} site and NH_4^+ site, in CAS crystal. We employ two theoretical methods: the superposition model (SPM) [11–13] and the fourth-order perturbation formulae on the basis of the dominant spin–orbit coupling mechanism [14]. The outcomes of both methods are consistent with the experimental results and they support earlier suggestions [5–7] that Mn^{2+} ions substitute for Cd^{2+} ions in CAS crystal.

2. Crystal structure

CAS crystal has cubic symmetry with the space group $P2_13$ (T^4) and contain four formula units per unit cell at room temperature. The cubic lattice parameters were reported to be a = 1.0350 nm [3,2] and 1.0362 nm [6]. Positional parameters and thermal parameters of CAS at room temperature were reported in [2,6]. Single unit cell of CAS is shown in Fig. 1 with the orientation of the crystallographic axes a, b, and c. The body diagonal of the cubic unit cell is parallel to the symmetry Z-axis [5] (see Fig. 1). CAS undergoes a first-order phase transition from the high-temperature cubic phase ($P2_13$) to the low-temperature monoclinic phase ($P2_1$) [2,15]. CAS is isomorphous to the langbeinite $K_2Mg_2(SO_4)_3$. The NH_4^+ and Cd^{2+} lie on the threefold axes, and the SO_4 tetrahedra are in general positions [8].

* Tel.: +90 212 3810307; fax: +90 212 3810300.
E-mail address: macikgoz@bahcesehir.edu.tr

0925-8388/$ – see front matter © 2011 Elsevier B.V. All rights reserved.
doi:10.1016/j.jallcom.2011.07.071

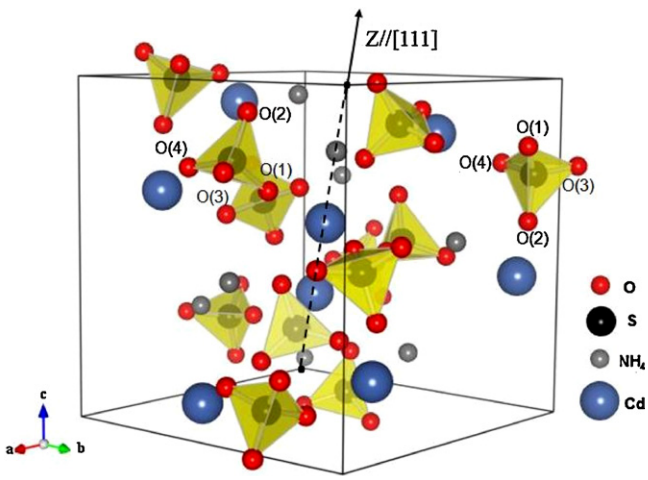

Fig. 1. Unit cell of $Cd_2(NH_4)_2(SO_4)$ (CAS) crystal. Orientation of the crystallographic axes *a*, *b*, and *c* and the symmetry axis (*Z*-axis) parallel to the body diagonal of the cubic unit cell are shown.

Table 1
Bond distances and coordination angles of ligands used for SPM calculations of ZFS parameters for Mn^{2+} ions at Cd^{2+} site in CAS.

Host Cd sites		Substitutional sites		Angle
Metal-oxygen	R_{hi} (nm)	Dopant Mn^{2+}-oxygen	R_i (nm)	θ_i (°)
Cd-O(1)	0.382873	Mn-O(1)	0.368873	46.7902
Cd-O(2)	0.425824	Mn-O(2)	0.411824	36.0849
Cd-O(3)	0.451958	Mn-O(3)	0.437958	64.8707
Cd-O(4)	0.224573	Mn-O(4)	0.210573	59.8448

Table 2
Bond distances and coordination angles of ligands used for SPM calculations of ZFS parameters for Mn^{2+} ions at $NH_4{}^+$ site in CAS.

Host NH_4 sites		Substitutional sites		Angle
Metal-oxygen	R_{hi} (nm)	Dopant Mn^{2+}-oxygen	R_i (nm)	θ_i (°)
NH_4-O(1)	0.367858	Mn-O(1)	0.327358	49.3410
NH_4-O(2)	0.29626	Mn-O(2)	0.25576	57.8399
NH_4-O(3)	0.513286	Mn-O(3)	0.472786	52.8615
NH_4-O(4)	0.434782	Mn-O(4)	0.394282	26.5269

3. Theoretical analysis

3.1. The coordinates of the ligand ions

The bond distances and corresponding coordination angles of ligands have been determined and tabulated for host Cd site in Table 1 and for host NH_4 site in Table 2. The distance of a ligand is usually different from the cation–anion distance in the host lattice because of the mismatch of the radius of the substitution atom r_s and that of the host atom r_h. Ligand distance can be reasonably approximated using the following formula [16]: $R_i \approx R_{hi} + (1/2)(r_s - r_h)$, where R_i and R_{hi} represent the ligand and cation–anion distances, respectively. Using the data: $r_i(Mn^{2+}) = 0.067$, $r_h(Cd^{2+}) = 0.092$ [17], and $r_h(NH_4{}^+) = 0.148$ [18] (in nm), and the cation–anion distances in Tables 1 and 2 yield R_i values given in Tables 1 and 2.

3.2. Superposition model analysis

Experimental spectra of Mn^{2+} doped CAS can be analyzed by utilizing the spin Hamiltonian, suitable for the spin $S = 5/2$ systems at trigonal type I symmetry sites (D_3, C_{3v}, D_{3d}), consisting of the Zeeman electronic terms and the ZFS terms (without considering the hyperfine terms) [19–22]:

$$H = \mu_B \boldsymbol{B} \cdot \boldsymbol{g} \cdot \boldsymbol{S} + \sum f_k b_k^q O_k^q = g_\perp \mu_B (B_x S_x + B_y S_y) + g_\parallel \mu_B B_z S_z + f_k (b_2^0 O_2^0 + b_4^0 O_4^0 + b_4^3 O_4^3) \tag{1}$$

where $\boldsymbol{g}$ is the spectroscopic splitting factor, μ_B – Bohr magneton, $\boldsymbol{B}$ – the applied magnetic field, $\boldsymbol{S}$ – the effective spin operator, and b_k^q are ZFSPs associated with the extended Stevens operators O_k^q, whereas $f_k = 1/3$, and 1/60 are the scaling factors for $k = 2$, and 4, respectively [23,24].

ZFSPs in Eq. (1) can be estimated using SPM approach outlined recently in [25,26]. The explicit SPM expressions for ZFSPs for a fourfold coordinated $3d^5$ ion in the Mn-O_4 complex in CAS are derived as

$$D_{SPM} = b_2^0 = \frac{\bar{b}_2(R_0)}{2}\left[\left(\frac{R_0}{R_1}\right)^{t_2}(3\cos^2\theta_1 - 1) + \left(\frac{R_0}{R_2}\right)^{t_2}(3\cos^2\theta_2 - 1) + \left(\frac{R_0}{R_3}\right)^{t_2}(3\cos^2\theta_3 - 1) + \left(\frac{R_0}{R_4}\right)^{t_2}(3\cos^2\theta_4 - 1)\right] \tag{2}$$

$$b_4^0 = \frac{\bar{b}_4(R_0)}{8}\left[\left(\frac{R_0}{R_1}\right)^{t_4}(35\cos^4\theta_1 - 30\cos^2\theta_1 + 3) + \left(\frac{R_0}{R_2}\right)^{t_4}(35\cos^4\theta_2 - 30\cos^2\theta_2 + 3) + \left(\frac{R_0}{R_3}\right)^{t_4}(35\cos^4\theta_3 - 30\cos^2\theta_3 + 3) + \left(\frac{R_0}{R_4}\right)^{t_4}(35\cos^4\theta_4 - 30\cos^2\theta_4 + 3)\right] \tag{3}$$

$$b_4^3 = 35\bar{b}_4(R_0)[\left(\frac{R_0}{R_1}\right)^{t_4}\sin^3\theta_1\cos\theta_1 + \left(\frac{R_0}{R_2}\right)^{t_4}\sin^3\theta_2\cos\theta_2 + \left(\frac{R_0}{R_3}\right)^{t_4}\sin^3\theta_3\cos\theta_3 + \left(\frac{R_0}{R_4}\right)^{t_4}\sin^3\theta_4\cos\theta_4]$$

Two data sets [27,28] of the model parameters, i.e. the intrinsic parameters $\bar{b}_k(R_0)$ and the power law exponents t_k, suitable for Mn^{2+} in CAS exist in literature (Table 5). These sets were adopted in our calculations together with three values of the reference distance R_0 taken as: (a) $R_0 = a_0/4$, where a_0 is the lattice parameter, (b) R_0 values from [27,28] for Mn^{2+}, and (c) $R_0 \approx R_{avg}$ [29,30].

3.3. The fourth-order perturbation formula of ZFS parameter D

Second-rank ZFS parameter $b_2^0 = D$ can also be calculated using the fourth-order perturbation formula on the basis of the dominant spin–orbit coupling mechanism [14]

$$D_{PT} = b_2^0 = \frac{3\zeta^2}{70p^2d}(-B_{20}^2 - 21\zeta B_{20}) + \frac{\zeta^2}{126p^2g}(-10B_{40}^2 + 7B_{43}^2) \tag{4}$$

with

$$p = 7B + 7C \qquad g = 10B + 5C \qquad d = 17B + 5C \tag{5}$$

where B and C are the Racah parameters. B_{kq} are the crystal-field parameters (CFPs) in Wybourne notation. They can be expressed using the superposition model as [14,31]:

$$B_{kq} = \sum_j \bar{A}_k(R_j) K_{kq}(\theta_j, \phi_j) \tag{6}$$

Table 3
Electrostatic parameters, spin–orbit coupling coefficient, cubic crystal-field parameter, and orbital reduction factor of Mn^{2+} ion at room temperature.

B_0	C_0	ζ_0	B	C	ζ	Dq	$k \approx N^2$
960 [44,45]	3325 [44,45]	347 [44,45]	690 [43]	3600 [43]	327.8[a] 300 [6]	1100[a] 1010 [43] 900 [6]	0.944[a]

[a] This study.

Table 4
ZFS parameters for Mn^{2+}:CAS crystal at room temperature.

Original ZFSPs			Ref.	Converted ZFSPs in units of [10^{-4} cm^{-1}]		
b_2^0	b_4^0	b_4^3		b_2^0	b_4^0	b_4^3
4850 ± 20 GHz	50 ± 10 GHz	−300 ± 200 GHz	[7]	161.83 ± 0.67	1.67 ± 0.33	−10.01 ± 6.67
−4719 ± 4 GHz	45 ± 30 GHz	2160 ± 1070 GHz	[5]	−157.46 ± 0.13	1.50 ± 1	72.07 ± 35.7
−171 ± 5 G (site 1)	−1.43 ± 0.1 G	–	[6]	−159.7 ± 0.5	−1.34 ± 0.1	–
−162 ± 5 G (site 2)	−1.60 ± 0.1 G	–		−151.3 ± 0.5	−1.49 ± 0.1	–

Table 5
The adopted SPM parameters and the calculated ZFSPs b_k^q (in 10^{-4} cm^{-1}) for the Mn^{2+} ions at the Cd^{2+} and $NH_4{}^+$ sites in CAS.

Model parameters (MP)	Set (*i*) [27]	Set (*ii*) [27]
t_2	8	8
t_4	14	14
$\bar{b}_2(R_0)$	−260	250 ± 20
$\bar{b}_4(R_0)$	0.8	0.7 ± 3
R_0 (for $\bar{b}_2$) (nm)	0.2200	0.2101
R_0 (for $\bar{b}_4$) (nm)	0.2150	0.2000

ZFS parameters for Mn^{2+} ions at Cd^{2+} sites

ZFSPs		b_2^0		b_4^0		b_4^3	
MP sets		*i*	*ii*	*i*	*ii*	*i*	*ii*
Calc.[a]	*	94.2	−90.5	−1.7	−1.5	66.1	57.8
	**	**158.9**	**−152.8**	**−4.2**	**−3.7**	**162.8**	**142.4**
Calc.[b]	*	25.7	−17.1	−0.1	−0.04	4.9	1.6
	**	43.4	−28.9	−0.3	−0.1	12.2	3.9
Calc.[c]	*	1693.0	−1627.9	−267.3	−233.9	10,377.8	9080.6
	**	2857.3	−2747.4	−658.1	−575.9	25,550.0	22,356.2

ZFS parameters for Mn^{2+} ions at $NH_4{}^+$ sites

		b_2^0		b_4^0		b_4^3	
MP sets		*i*	*ii*	*i*	*ii*	*i*	*ii*
Calc.[a]	*	1.6	−1.5	−0.04	−0.04	1.42	1.24
	**	9.6	−9.3	−0.33	−0.29	10.94	9.58
Calc.[b]	*	0.42	−0.28	−0.003	−0.001	0.11	0.03
	**	2.6	−1.75	−0.02	−0.008	0.82	0.26
Calc.[c]	*	27.9	−26.9	−6.7	−5.9	222.7	194.9
	**	172.9	−166.3	−51.6	−45.2	1717.9	1503.2

[a] R_0 is chosen to be $a_0/4 \approx 0.25875$ nm.
[b] R_0 as adopted earlier in their source papers (set (*i*) and set (*ii*)).
[c] Based on the approximation $R_0 \approx R_{avg} = 0.3713$.

* Calculations on host crystal structure data.
** Calculations based on the contribution from the mismatch of the radii of substitution atom r_s and host atom r_h.

where $K_k^q(\theta_i, \phi_i)$ are the coordination factors which are functions of the position angles θ_i and ϕ_i of ligands. Here it should be noted that the coordination factors expressed in the Wybourne notation should be distinguished from those in the extended Stevens operator notation [32], which are used to derive the SPM expressions for ZFSPs. For a discussion of the intricate aspects involved in the SPM equations expressed in the two notations, the readers may consult the recent paper [33]. $\bar{A}_k(R_j)$ are the intrinsic parameters and they obey the following power law: $\bar{A}_k(R_j) = \bar{A}_k(R_0)(R_0/R_j)^{t_k}$. R_0 and R_i are the reference distance and the distance of the ith ligand, respectively. t_k are the power-law exponents.

The explicit SPM expressions for the CFPs B_{kq} of Mn^{2+} ion at the Cd^{2+} and NH^{4+} sites in CAS have the same mathematical structure with the SPM equations for ZFSPs derived as in the previous section. Intrinsic parameter $\bar{A}_4$ for CFPs B_{40} and B_{43} can be estimated from the cubic CFP Dq from the relation [14]:

$$Dq = -\frac{3}{14}\bar{A}_4[(35\cos^4\theta_{avg} - 30\cos^2\theta_{avg} + 3) - 7\sqrt{2}\cos\theta_{avg}\sin^3\theta_{avg}] \quad (7)$$

where the averaged values $\theta_{avg} = 51.8977^\circ$ for Cd^{2+} site and $\theta_{avg} = 46.6423^\circ$ for $NH_4{}^+$ site were adopted. Thus, we obtain

$Dq = 1.35\bar{A}_4$ for Mn^{2+} at Cd^{2+} site, whereas for $NH_4{}^+$ site $Dq = 1.28\bar{A}_4$. The well-known ratio $\bar{A}_2(R_0)/\bar{A}_4(R_0) \approx 10.8$ for iron group ions in several crystals [34–36] is also used. The following values are adopted: $t_2 = 3$, $t_4 = 5$ as the most common ones in many studies, e.g. [37,38]. Due to the covalence reduction effect for $3d^n$ ions in crystals both electrostatic parameters B, C and the spin–orbit coupling parameter ζ are smaller than the corresponding free-ion values (B_0, C_0, and ζ_0) [39,40]. Orbital reduction factor can be determined from the relation $N^2 \approx \left(\sqrt{B/B_0} + \sqrt{C/C_0}\right)/2$ and then the spin–orbit coupling parameter is evaluated by $\zeta \approx N^2\zeta_0 \approx k$ [41,42]. All relevant parameters adopted for CAS:Mn^{2+} system [43] at room temperature are tabulated in Table 3.

4. Results and discussion

The experimental values in the original units and the corresponding ones reconverted to units of $(10^{-4})\,cm^{-1}$ are given in Table 4. Using Eqs. (2) and (3), SPM calculations were performed considering contributions from the four O^{-2} ligands around Mn^{2+} ions substituting at the Cd^{2+} and NH^{4+} sites.

The ZFSPs predicted for Mn^{2+} ions using two modeling approaches, the host crystal structure data (*) and contributions from the mismatch of the radii of the substitution (r_s) and host atom (r_h) (**), are listed in Table 5. Comparison of the ZFSPs calculated by SPM (Table 5) with the experimental values (Table 4), indicates that Mn^{2+} ions locate at the Cd^{2+} sites. The best values of ZFSPs are obtained when the reference distance R_0 is chosen to be $a_0/4$. Generally, taking into account the contribution from the mismatch in radii of the substitution and host atoms yields better results.

There were some inconsistencies for the signs of ZFSPs and the value of b_4^3 in the experimental data of Mn^{2+}:CAS (see Table 4). A discrepancy concerning the experimental sign of $b_2^0(= D)$ exists in the literature; positive in [7] but negative in [5,6]. It was pointed out in [6] that the sign of D and (a-F) was relative, however, the sign of D was supposed negative from a point-charge calculation [46,47]. That is why we utilized two model parameter (MP) sets – they yield similar qualitative results but opposite sign of b_2^0. The first MP set (i) with negative $\overline{b_2}$ yields positive b_2^0, whereas the second MP set (ii) with positive $\overline{b_2}$ results in negative b_2^0. For the fourth-rank ZFSPs both MP sets yield the same signs; negative for b_4^0 and positive for b_4^3. The modeling approach which yields the best result for b_2^0 (bold line in Table 5), results in b_4^q differing from the experimental values. However, by just varying $\bar{b}_4$ to $0.34 \times 10^{-4}\,cm^{-1}$ using the flexibility in MP set (ii), we obtain $b_4^0 = -1.78 \times 10^{-4}\,cm^{-1}$ and $b_4^3 = 69.2 \times 10^{-4}\,cm^{-1}$, which are in good agreement with the results of [5] (see Table 4). Hence, for Mn^{2+} ions in langbeinite-type crystals, $\bar{b}_4 = 0.34 \times 10^{-4}\,cm^{-1}$ with $t_4 = 14$ seem reasonable.

The results of SPM analysis reveal clearly that Mn^{2+} ions can replace Cd^{2+} ions in CAS crystal. In order to confirm this finding and clarify the discrepancy in the sign of b_2^0, we also derive the second-rank ZFS parameter $b_2^0(= D)$ using the fourth-order perturbation theory (PT) formula [14]. Hence, the crystal-field (CF) parameters and the zero-field splitting (ZFS) parameter D_{PT} relevant to the Mn^{2+} ions in tetrahedral coordination at both Cd^{2+} and $NH_4{}^+$ sites in CAS crystal have been calculated (Table 6).

PT calculations yield positive D. Two cubic CF parameter Dq for Mn^{2+}:CAS exist in literature (see Table 3). This makes us consider Dq as an adjustable parameter. In PT calculations we used $Dq = 1010\,cm^{-1}$ [43], which results in a bit lower D value than the experimental ones. Taking $Dq = 1100\,cm^{-1}$, we obtain D_{PT} close to the experimental values. Also, it is worth to consider how the changes in Dq affect the ZFSP D. Fig. 2 shows a clear linear relationship between D_{PT} and Dq at both sites. For comparison, the calculated D_{SPM} and D_{PT} values for Mn^{2+} at Cd^{2+} and $NH_4{}^+$ sites are tabulated in Table 7 together with the experimental D_{exp}.

Table 6
Calculated the ZFS parameter D_{PT} (in $10^{-4}\,cm^{-1}$) and CF parameters (in cm^{-1}) for Mn^{2+} ion at the Cd^{2+} (upper part) and $NH_4{}^+$ (lower part) sites in CAS.

		D_{PT}	B_{20}	B_{40}	B_{43}
Calc.[a]	*	80.12	−946.1	−4073.9	−6459.5
	**	**139.0**	**−1351.3**	**−5525.7**	**−8794.3**
For $Dq = 1100\,cm^{-1}$		**161.62**	**−1471.7**	**−6020.7**	**−9582.0**
Calc.[b]	*	25.3	−581.5	−1810.2	−2870.2
	**	40.6	−830.6	−2455.3	−3907.6
Calc.[c]	*	2231	−2795.6	−24,787.0	−39,303.0
	**	4141	−3992.9	−33,621.0	−53,509.0
Calc.[a]	*	−81.2	2579.4	−1545.5	−2137.9
	**	−102.7	3334.0	−3075.5	−4245.3
For $Dq = 1100\,cm^{-1}$		−113.69	3631.0	−3348.4	−4621.9
Calc.[b]	*	−46.8	1585.4	−686.7	−949.9
	**	−61.3	2049.3	−1366.6	−1886.3
Calc.[c]	*	−227	7621.7	−9403.7	−13,008.0
	**	0.00059	9851.6	−18,713.0	−25,830.0

The notes (a) to (c) and *, ** have the same meaning as in Table 5.

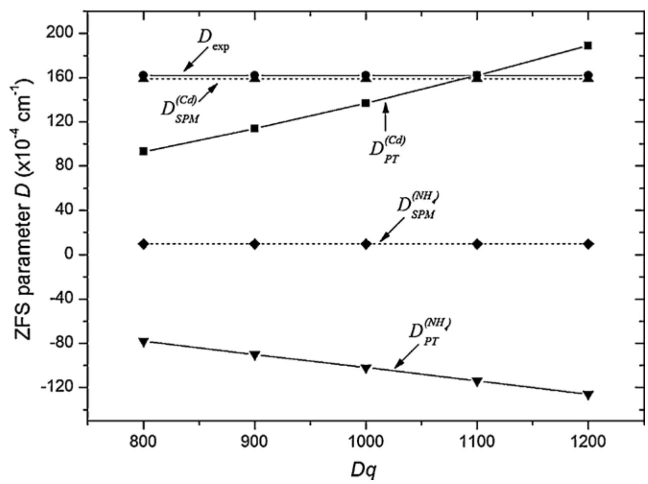

Fig. 2. Variation of ZFS parameter D_{PT} at both Cd^{2+} and $NH_4{}^+$sites versus the cubic crystal-field parameter Dq for Mn^{2+} centers in CAS.

Table 7
Comparison of the calculated D_{SPM} and D_{PT} with the experimental D_{exp} for Mn^{2+} ions at Cd^{2+} and $NH_4{}^+$ sites in CAS; all parameters in $(10^{-4}\,cm^{-1})$.

D parameter	Cd^{2+} sites	NH^{4+} sites
D_{SPM}	158.9	9.6
D_{PT}	161.62	−113.69
D_{exp} [7]	161.83 ± 0.67	
D_{exp} [5]	−157.46 ± 0.13	
D_{exp} [6]	−159.7 ± 0.5	

5. Conclusion

Zero-field splitting (ZFS) parameters (ZFSPs) b_2^0 (=D) and b_4^q (q = 0, 3) of Mn^{2+} in CAS crystal have been investigated using superposition model (SPM) and crystallographic data at the substitutional Cd^{2+} and NH^{4+} sites. The SPM results on b_2^0 (=D) were confirmed, and its sign was determined as positive utilizing the fourth-order perturbation formula on the basis of the dominant spin–orbit coupling mechanism. The ZFS parameters obtained for Mn^{2+} ion at Cd^{2+} site using both approaches are in good agreement with the experimental values. Hence, it is indicated theoretically that Mn^{2+} ions substitute for the Cd^{2+} ions in CAS crystal in addition to experimental suggestions.

Acknowledgement

The present work was supported by the Research Fund from Bahcesehir University.

References

[1] K.H. Hellwege, A.M. Hellwege (Eds.), Landolt-Börnstein, III/16b, Springer-Verlag, Berlin, Heidelberg, New York, 1982.
[2] C. Moriyoshi, E. Magome, K. Itoh, Ferroelectrics 337 (2006) 85.
[3] F. Jona, R. Pepinsky, Phys. Rev. 103 (1956) 1126.
[4] S. Kreske, V. Devarajan, J. Phys. C 15 (1982) 7333.
[5] I. Tatsuzaki, J. Phys. Soc. Jpn. 17 (1962) 582.
[6] H.K. Ng, C. Calvo, Can. J. Chem. 53 (1975) 1449.
[7] S.K. Misra, S.Z. Korczak, J. Phys. C 19 (1986) 4353.
[8] D.S. Babu, G.S. Sastry, M.D. Sastry, A.G.I. Dalvi, J. Phys. C 17 (1984) 4245.
[9] D.S. Babu, G.S. Sastry, M.D. Sastry, A.G.I. Dalvi, Phase Trans. 15 (1989) 11.
[10] C.A. McDowell, P. Raghunathan, R. Srinivasan, Mol. Phys. 29 (1975) 815.
[11] D.J. Newman, W. Urban, Adv. Phys. 24 (1975) 793.
[12] D.J. Newman, B. Ng, Rep. Prog. Phys. 52 (1989) 699.
[13] M. Andrut, M. Wildner, C. Rudowicz, in: A. Beran, E. Libowitzky (Eds.), Spectroscopic Methods in Mineralogy – European Mineralogical Union Notes in Mineralogy, vol. 6, Eötvös University Press, Budapest, 2004, p. 145 (Ch. 4).
[14] W.L. Yu, M.G. Zhao, Phys. Rev. B 37 (1988) 9254.
[15] H. Ohshima, E. Nakamurja, Phys. Chem. Solids 27 (1966) 481.
[16] W.C. Zheng, Physica B 215 (1995) 255.
[17] R.D. Shannon, C.T. Prewitt, Acta Crystallogr. B 26 (1970) 1046.
[18] T. Akutagawa, T. Nakmaura, T. Inabe, A.E. Underhill, Synth. Metals 86 (1–3) (1997) 1861.
[19] A. Abragam, B. Bleaney, Electron Paramagnetic Resonance of Transition Ions, Clarendon Press, Oxford, 1970;
A. Abragam, B. Bleaney, Electron Paramagnetic Resonance of Transition Ions, Dover, New York, 1986.
[20] S. Altshuler, B.M. Kozyrev, Electron Paramagnetic Resonance in Compounds of Transition Elements, Wiley, New York, 1974.
[21] C. Rudowicz, Magn. Reson. Rev. 13 (1987) 1, Erratum: C. Rudowicz, Magn. Res. Rev. 13 (1987) 335.
[22] C. Rudowicz, S.K. Misra, Appl. Spectrosc. Rev. 36 (2001) 11.
[23] C. Rudowicz, J. Phys. C18 (1985) 1415, Erratum: ibidem C 18 (1985) 3837.
[24] C. Rudowicz, C.Y. Chung, J. Phys. Condens. Matter 16 (2004) 5825.
[25] P. Gnutek, M. Açıkgöz, C. Rudowicz, Opt. Mater. 32 (2010) 1161.
[26] M. Açıkgöz, P. Gnutek, C. Rudowicz, Solid State Commun. 150 (2010) 1077.
[27] D.J. Newman, E. Siegel, J. Phys. C 9 (1976) 4285.
[28] Vishwamittar, S.P. Puri, J. Chem. Phys. 61 (1974) 3720.
[29] K.A. Müller, W. Berlinger, J. Phys. C: Solid State Phys. 16 (1983) 6861.
[30] X.X. Wu, W.L. Feng, W.C. Zheng, Phys. Stat. Sol. (b) 244 (2007) 3347.
[31] D.J. Newman, Adv. Phys. 20 (1970) 197.
[32] C. Rudowicz, J. Phys. C: Solid State 20 (1987) 6033.
[33] M. Karbowiak, C. Rudowicz, P. Gnutek, Opt. Mater. 33 (2011) 1147–1161.
[34] D.J. Newman, D.C. Pryce, W.A. Runciman, Am. Miner. 63 (1978) 1278.
[35] Z.Y. Yang, J. Phys.: Condens. Matter 12 (2000) 4091.
[36] M. Acikgoz, Spectrochim. Acta A 78 (2011) 273.
[37] W.L. Yu, Phys. Rev. B 41 (1990) 9415.
[38] W.C. Zheng, Q. Zhou, X.X. Wu, Y. Mei, Spectrochim. Acta A 63 (2006) 126.
[39] M.G. Zhao, J.A. Xu, G.R. Bai, H.S. Xie, Phys. Rev. B 27 (1983) 1516.
[40] Z.Y. Yang, C. Rudowicz, J. Qin, Physica B 318 (2002) 188.
[41] D. Curie, C. Barthon, B. Canny, J. Chem. Phys. 61 (1974) 3048.
[42] C.X. Zhang, X.Y. Kuang, G.D. Li, H. Wang, Chem. Phys. Lett. 441 (2007) 143.
[43] M. Morita, N. Sakuta, J. Luminesc. 18/19 (1979) 801.
[44] J.S. Griffith, The Theory of Transition-Metal Ions, Cambridge University Press, London, 1961.
[45] L.E. Orgal, J. Chem. Phys. 23 (1955) 1819.
[46] C.A. Morrison, Crystal Fields for Transition-Metal Ions in Laser Host Materials, Springer, Berlin, 1992.
[47] M.T. Hutchings, Solid State Phys. 16 (1964) 227.